Active OB stars: structure, evolution, mass loss, and critical limits
Proceedings IAU Symposium No. 272, 2010
C. Neiner, G. Wade, G. Meynet & G. Peters, eds.

doi:10.1017/S1743921311011112

Radial and nonradial oscillations of massive supergiants

Hideyuki Saio

Astronomical Institute, Graduate School of Science, Tohoku University,
Sendai, Miyagi 980-8578, Japan
email: saio@astr.tohoku.ac.jp

Abstract. Stability of radial and nonradial oscillations of massive supergiants is discussed. The kappa-mechanism and strange-mode instability excite oscillations having various periods in wide ranges of the upper part of the HR diagram. In addition, in very luminous ($\log L/L_\odot \gtrsim 5.9$) models, monotonously unstable modes exist, which probably indicates the occurrence of optically thick winds. The instability boundary is not far from the Humphreys-Davidson limit. Furthermore, it is found that there exist low-degree ($\ell = 1, 2$) oscillatory convection modes associated with the Fe-opacity peak convection zone, and they can emerge to the stellar surface so that they are very likely observable in a considerable range in the HR diagram. The convection modes have periods similar to g-modes, and their growth-times are comparable to the periods. Theoretical predictions are compared with some of the supergiant variables.

Keywords. stars: oscillations (including pulsations), supergiants, instabilities, convection

1. Introduction

Light and velocity variations on various time-scales are common in very luminous stars (e.g., van Genderen 1989, van Leeuwen *et al.* 1998). Those variations are caused by various kinds of instabilities. Here we discuss mainly the cause of microvariations of massive supergiants based on linear stability analyses applied to evolutionary models of massive stars. The evolution models were calculated by a Henyey-type code using OPAL opacity tables (Iglesias & Rogers 1996). Wind mass-loss is included for the evolutionary models for $M_i \gtrsim 30 M_\odot$ ($M_i =$ initial mass) based on the mass-loss rates of Vink *et al.* (2001). Linear stability analyses were performed using the methods given in Saio, Winget & Robinson (1983) for radial modes and Saio & Cox (1980) for nonradial modes, where the outer mechanical boundary condition was modified to $\delta P_{\rm gas} \to 0$ ($\delta P_{\rm gas}$ means the Lagrangean perturbation of gas pressure) taking into account the fact that radiation pressure is dominant near the outer boundary. It should be noted, however, that the effect of winds on radial and nonradial oscillations is not included because the effect is not well understood yet.

2. Stability of radial modes

Figure 1 shows instability boundaries of spherical symmetric modes and selected evolutionary tracks. Short-dashed line indicates the instability boundary for low-order modes. The nearly vertical "finger" ($4.4 \gtrsim \log T_{\rm eff} \gtrsim 4.3$) is the well-known β Cep instability strip, in which low-order radial modes and nonradial p-modes are excited by the kappa-mechanism at the Fe-peak of opacity around $T \sim 2 \times 10^5$K. At the luminous part of the instability strip, the cool-side boundary bents to become horizontal around $\log(L/L_\odot) \sim 5.8$. This is due to the strange-mode instability which occurs in models with sufficiently high luminosity to mass ratios as $L/M \gtrsim 10^4 L_\odot/M_\odot$. The properties of

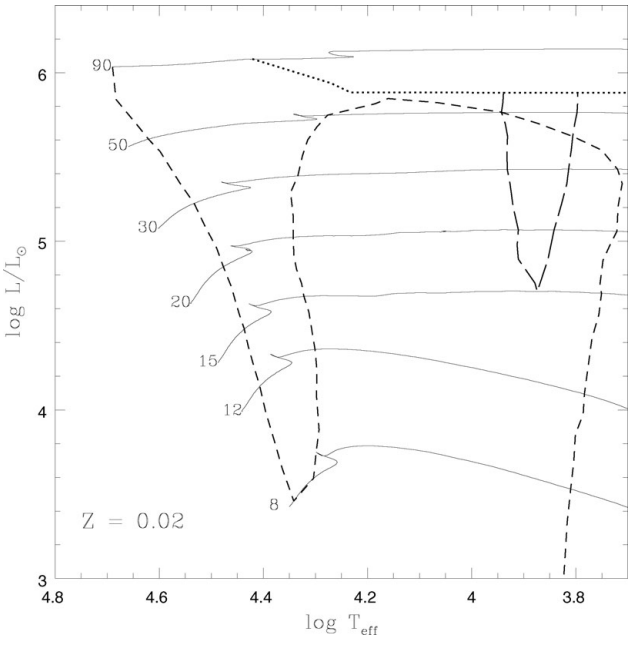

Figure 1. Instability boundaries of radial modes and selected evolutionary tracks. Short- and long-dashed lines indicate stability boundaries for low-order and relatively high-order radial modes, respectively. Dotted line indicates the boundary for monotonously unstable radial modes. Numbers along evolutionary tracks indicate initial masses in solar units. The instability boundaries for radial modes also represent approximately the boundaries for low-degree ($\ell \lesssim 2$) nonradial p-modes.

the strange modes have been investigated by e.g., Glatzel & Kiriakidis (1993), Glatzel (1994), Saio, Baker & Gautschy (1998) (see also Saio 2009).

Nearly vertical part of the boundary around $\log T_{\rm eff} \sim 3.8$ indicates the well-known blue edge of the Cepheid instability strip. (Red edge is not obtained because the perturbation of convective flux is neglected in this analysis.)

In the vertical narrow region indicated by long-dashed line around $\log T_{\rm eff} \sim 3.9 - 3.8$, relatively high-order radial modes are excited around hydrogen ionization zone. (Low-degree nonradial modes with similar frequencies are also excited.) The amplitude of these modes are extremely confined to the outermost layers above the hydrogen ionization zone. Since these modes exist even under the NAR approximation where thermal-time is set to be zero (Gautschy & Glatzel 1990), they may be classified as strange modes. These modes have got little attention so far (cf. Gautschy 2009).

Dotted line in Fig. 1 shows the boundary above which monotonously unstable modes exist. The growth times of these modes are much shorter than the timescale of evolution. The presence of such monotonously unstable modes have not been recognized before. Such a mode probably corresponds to the presence of an optically thick wind as investigated by Kato & Iben (1992) for WR stars. It is interesting to note that the boundary is not far from the Humphreys-Davidson limit (Humphreys & Davidson 1979).

3. Stability of nonradial modes

The instability ranges of low-degree high-order g-modes are shown in Fig. 2 by solid and dotted lines for $\ell = 2$ and $\ell = 1$ modes, respectively. These modes are excited by the kappa-

https://doi.org/10.1017/S1743921311011112 Published online by Cambridge University Press

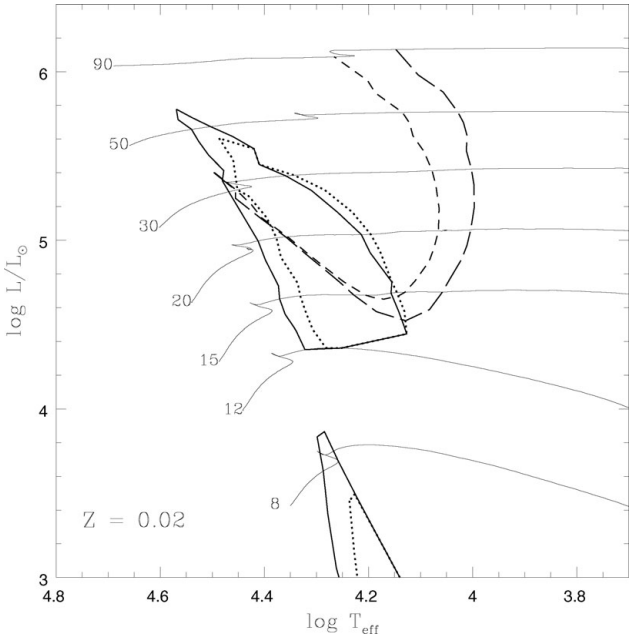

Figure 2. Ranges where nonradial oscillations are expected to be detected. The instability boundaries for SPB-type low-degree high-order g-modes are shown by solid ($\ell = 2$) and dotted ($\ell = 1$) lines. The ranges where oscillatory convection modes should be observable are indicated by long- and short-dashed lines for $\ell = 1$ and $\ell = 2$, respectively.

mechanism at the Fe opacity peak. They are responsible for the long-period variations in slowly pulsating B (SPB) stars. Such g-modes can be excited even in supergiants (SPBsg) because a shell convection zone associated with hydrogen burning reflects some g-modes and hence suppresses dissipation otherwise expected in the core (Saio *et al.* 2006).

The long dashed and short dashed lines in Fig. 2 indicate ranges where oscillatory convection modes of $\ell = 1$ and $\ell = 2$, respectively, are expected to be observable. It is well known that linear convection modes are monotonously (dynamically) unstable in *adiabatic analyses*. Shibahashi & Osaki (1981) found, however, that the high-degree ($\ell \geqslant 10$) convection modes become overstable (oscillatory) when the nonadiabatic effect is included in luminous ($L/L_\odot = 10^5$) models hotter than the cepheid instability strip.

In our massive star models, it is found that low-degree ($\ell \leqslant 2$) oscillatory convection modes exist associated with the Fe-opacity peak convection zones, and some of these modes are expected to be observable. Since the growth time of a convection mode is short (comparable to the period), the mode is expected to have a large amplitude in the convective zone. Therefore, the visibility of the oscillatory convective modes can be measured by the ratio of the photospheric amplitude to the maximum amplitude in the interior (mostly in the convection zone). Assuming that an oscillatory convection mode is observable when the ratio is larger than 0.2, the boundaries of the visible ranges are shown in Fig. 2 by dashed lines. Oscillatory convection modes are visible in sufficiently luminous ($\log L/L_\odot \gtrsim 4.6$) B-type stars. Although there are many oscillatory convection modes in a star, only one or two modes for a given ℓ are visible because the other modes are well confined to the convection zone. Periods of these modes are comparable to g-modes much longer than those of radial modes. These oscillatory convection modes might be responsible for long-period variations in supergiant stars.

https://doi.org/10.1017/S1743921311011112 Published online by Cambridge University Press

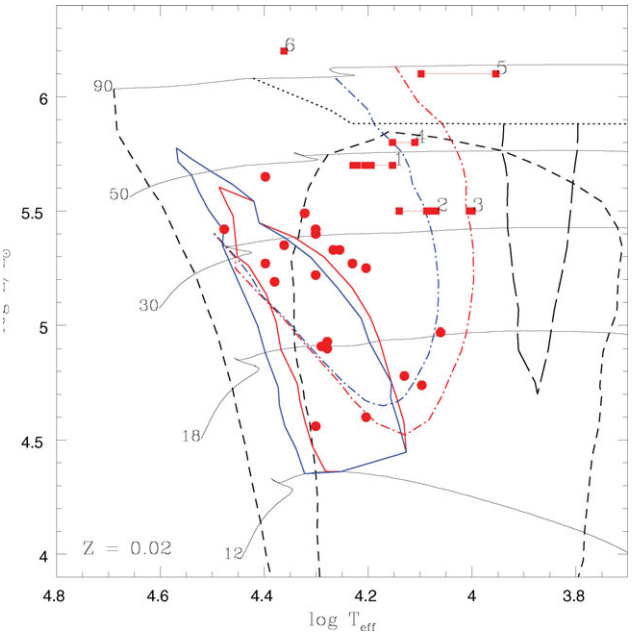

Figure 3. Ranges where (quasi-)periodic variable stars are expected on the HR diagram are compared with supergiant variables analyzed by Lefever *et al.* (2007) (big filled circles) and LBVs by Lamers *et al.* (1998) (filled squares). Positions at different LBV (or S Dor) phases for each star are connected with thin lines; 1 = R 712, 2 = HR Car, 3 = 164 G Sco, 4 = S Dor, 5 = R 1273, 6 = AG Car.

4. Comparison with supergiant variables

Observed positions of variable supergiants on the HR diagram are compared with the instability and visibility boundaries in Fig. 3. Their periods-$T_{\rm eff}$ relations are compared with theoretical ones in Figs. 4 and 5. Fig. 3 indicates that all the hotter ($\log T_{\rm eff} \gtrsim 4$) and luminous ($\log L/L_{\odot} \gtrsim 4.5$) stars are expected to show (quasi-)periodic variations, which is consistent with the observational fact that no or at most a very little number of stable supergiants exist in a spectral range of O9 – A0 as found by van Genderen (1989).

Big dots in Fig. 3 are relatively less luminous supergiant variables analyzed by Lefever *et al.* (2007). This figure indicates most of them to have masses ranging from $\sim 15M_{\odot}$ to $\sim 30M_{\odot}$. They are located on the HR diagram in the g-mode instability regions or visible range of oscillatory convection modes. Fig. 4 compares the periods of these stars as function of the effective temperature with theoretical ones of $15M_{\odot}$ and $30M_{\odot}$ models. This figure indicates that for most of these stars periods seem consistent to low-degree high-order g-modes (SPBsg) or oscillatory convection modes. We note, however, that for the coolest three stars the periods are shorter than any of the excited modes. Although these three stars are located on the HR diagram in the region where oscillatory convection modes should be visible (Fig. 3), the periods are much shorter than those of the oscillatory convection modes. If these effective temperatures are accurate, an unknown excitation mechanism might be working in these stars.

Fig. 5 compares theoretical periods of very massive models ($M_i = 50M_{\odot}$ and $70M_{\odot}$) with periods of microvariations of some LVB stars analyzed by Lamers *et al.* (1998), each of which has different periods and effective temperature depending on the LBV (S Dor) phases. Figs. 5 and 3 indicate that the microvariations of R 712 (1), S Dor (4) and AG Car (6) are consistent to the properties of oscillatory convection modes.

https://doi.org/10.1017/S1743921311011112 Published online by Cambridge University Press

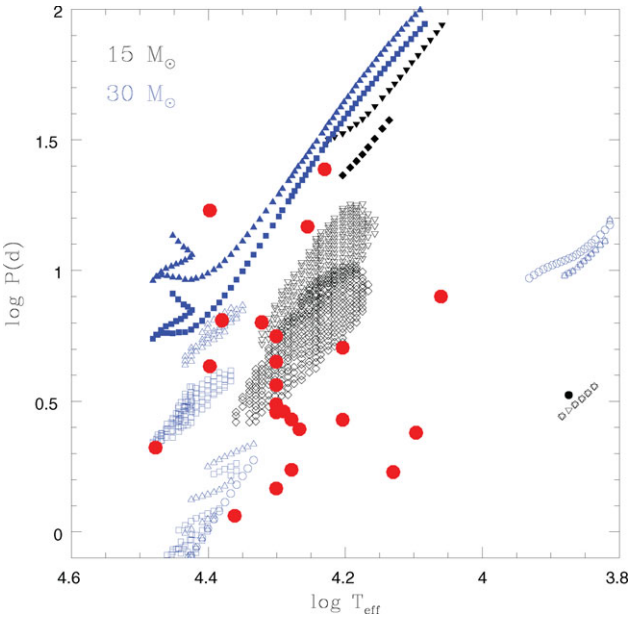

Figure 4. Periods of excited modes and of observable oscillatory convection modes versus effective temperature, where open ($30M_\odot$) and filled ($15M_\odot$) circles are radial modes; triangles ($30M_\odot$) and inverted triangles ($15M_\odot$) are $\ell = 1$ modes; squares ($30M_\odot$) and diamonds ($15M_\odot$) are $\ell = 2$ modes. Convection modes are shown by filled symbols for nonradial modes. Big dots show observed periods-$T_{\rm eff}$ relations of supergiants from Lefever *et al.* (2007).

The periods of microvariations of HR Car (2), 164 G Sco (3), and AG Car (5) are consistent with periods of strange modes. However, luminosities of HR Car and 164 G Sco are too low for the strange modes to exist (Fig. 3). Further investigations are needed to resolve the discrepancy.

5. Summary

We have discussed various instabilities that occur in massive supergiants. Radial modes and nonradial p- and g-modes are excited by the kappa-mechanism at the Fe opacity bump at $T \sim 2 \times 10^5$.

In a star with a very high luminosity to mass ratio of $L/M \gtrsim 10^4 L_\odot/M_\odot$, the strange mode instability works for radial and nonradial modes. Strange modes seem to be responsible for quasi-periodic variations in some of the luminous supergiants.

In addition, it is found that in very luminous models ($\log L/L_\odot \gtrsim 5.9$) a monotonously unstable radial mode exists, which is probably related to the occurrence of an optically thick wind. It is interesting to note that the instability boundary roughly coincides with the Humphreys-Davidson limit.

Furthermore, we found that low-degree ($\ell = 1, 2$) oscillatory convection modes exist in the convection zones caused by the Fe opacity peak, and that some of them can emerge to the stellar surface and hence be observable. The oscillatory convection modes have periods of $10 \sim 10^2$days depending of the effective temperature, which are longer than those of strange modes. The growth-times are comparable to the periods. They seem to be consistent with the properties of long-period microvariations in LVB stars (see Saio 2010 for further discussions).

https://doi.org/10.1017/S1743921311011112 Published online by Cambridge University Press

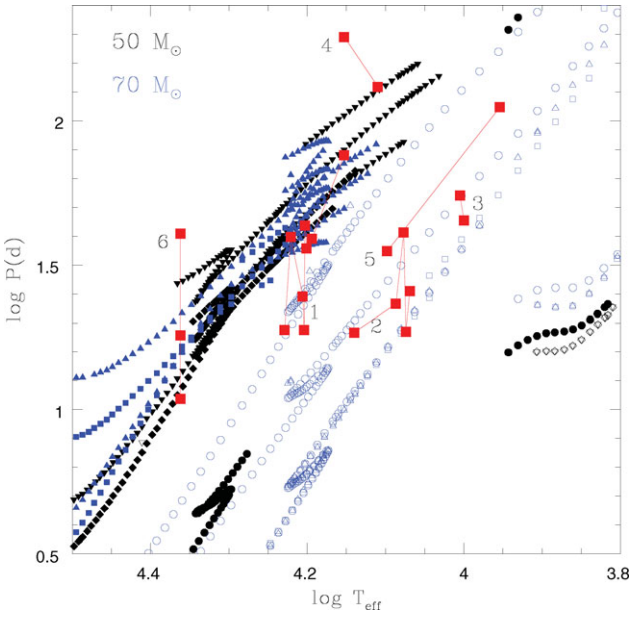

Figure 5. Theoretical periods of excited modes and of observable oscillatory convection modes versus effective temperature, where open ($70M_\odot$) and filled ($50M_\odot$) circles are radial modes; triangles ($70M_\odot$) and inverted triangles ($50M_\odot$) are $\ell = 1$ modes; and squares ($70M_\odot$) and diamonds ($50M_\odot$) are $\ell = 2$ modes. Convection modes are shown by filled symbols for nonradial modes. Big filled squares connected with thin lines show observed periods-$T_{\rm eff}$ relations of LBVs obtained by Lamers *et al.* (1998). Periods at different LBV (or S Dor) phases for each star are connected with thin lines; 1 = R 712, 2 = HR Car, 3 = 164 G Sco, 4 = S Dor, 5 = R 1273, 6 = AG Car.

References

Gautschy, A. 2009, *A&A*, 498, 273
Gautschy, A. & Glatzel, W. 1990, *MNRAS*, 245, 597
Glatzel, W. 1994, *MNRAS*, 271, 66
Glatzel, W., & Kiriakidis, M. 1993, *MNRAS*, 263, 375
Humphreys, R. M. & Davidson, K. 1979, *ApJ*, 232, 409
Iglesias, C. A. & Rogers, F. J. 1996, *ApJ*, 464, 943
Kato, M. & Iben, Jr., I. 1992, *ApJ*, 394, 305
Lamers, H. J. G. L. M., Bastiaanse, M. V., Aerts, C., & Spoon, H. W. W. 1998, *A&A*, 335, 605
Lefever, K., Puls, J., & Aerts, C. 2007, *A&A*, 463, 1093
Saio, H. 2009, *Communications in Asteroseismology*, 158, 245
Saio, H., 2010, *MNRAS*, accepted, arXiv:1011.4729
Saio, H., Baker, N. H., & Gautschy, A. 1998, *MNRAS*, 294, 622
Saio, H. & Cox, J. P. 1980, *ApJ*, 236, 549
Saio, H., Kuschnig, R., Gautschy, A., & Cameron, C. *et al.* 2006, *ApJ*, 650, 1111
Saio, H., Winget, D. E., & Robinson, E. L. 1983, *ApJ*, 265, 982
Shibahashi, H. & Osaki, Y. 1981, *PASJ*, 33, 427
van Genderen, A. M. 1989, *A&A*, 208, 135
van Leeuwen, F., van Genderen, A. M., & Zegelaar, I. 1998, *A&AS*, 128, 117
Vink, J. S., de Koter, A., & Lamers, H. J. G. L. M. 2001, *A&A*, 369, 574

https://doi.org/10.1017/S1743921311011112 Published online by Cambridge University Press